Yonago Acta Medica 2021;64(2):155–161 doi: 10.33160/yam.2021.05.002

Up-To-Date Magnetic Resonance Imaging Findings for the Diagnosis of Hypothalamic and Pituitary Tumors

Masamichi Kurosaki,* Makoto Sakamoto,* Atsushi Kambe* and Takafumi Ogura*
**Division of Neurosurgery, Department of Brain and Neurosciences, School of Medicine, Faculty of Medicine, Tottori University, Yonago 683-8504, Japan*

ABSTRACT
Magnetic resonance imaging (MRI) is the preferred imaging technique for the sellar and parasellar regions. In this review article, we report our clinical experience with MRI for hypothalamic and pituitary lesions, such as pituitary adenomas, craniopharyngiomas, Rathke cleft cysts, germinoma, and hypophysitis with reference to the histopathological findings through a review of the literature. Our previous study indicated that three dimensional-spoiled gradient echo sequence is a more suitable sequence for evaluating sellar lesions on postcontrast T1 weighted image (WI). This image demonstrates the defined relationship between the tumor and its surroundings, such as the normal pituitary gland, cavernous sinus, and optic pathway. We demonstrated the characteristic MRI findings of functioning pituitary adenoma. In growth hormone-producing adenoma, signal intensity on T2WI is important to differentiate densely from sparsely granulated somatotroph adenomas. In prolactin-producing pituitary adenomas, distinct hypointense areas in early phase on T2WI, possibly owning to diffuse hemorrhage, indicate pronounced regressions of invasive macroprolactinomas during cabergoline therapy. The two histopathological subtypes, adamantinomatous and squamous papillary craniopharyngioma, differ in genesis. Calcified tumors are mostly adamantinomatous type. On MRI, these lesions have a heterogenous appearance with a solid portion and cystic components. The solid portions and cyst wall enhance heterogeneously. Although cyst fluid of Rathke cleft cysts show variable intensities on MRI, intracystic waxy nodule can be hypointense on T2WI. The enhancing cyst wall may contain the squamous metaplasia. Cystic lesions of the sellar and parasellar areas may be difficult to differentiate on a clinical, imaging, or even histopathological basis.

Key words craniopharyngioma; pituitary adenoma; Rathke cleft cyst; three-tesla MRI

Magnetic resonance imaging (MRI) is the preferred imaging technique for the sellar and parasellar regions.[1, 2] Several different lesions occur around this area. High-field MRI is a recent advancement in medical imaging.[3–5] A three-tesla (3T) MRI unit was introduced into our hospital in December 2003. Recently, we have used two 3T MRI machines. At 3T, three dimensional (3D)-spoiled gradient echo (SPGR) sequence provided significantly better images than the spin-echo (SE) sequence in terms of the border of sellar lesions and delineation of the cranial nerves.[3]

A 3D-SPGR sequence has been used for the T1WI, and for the T2WI a fast SE sequence was routinely used for the diagnosis of the sellar lesions. In some cases, susceptibility WI[6] and/or arterial spin-labeled perfusion imaging (ASL) has been used. We advocated the 3T MRI state-of-the-art technique that provided significant assistance as a diagnostic and therapeutic tool for the treatment of hypothalamic and pituitary tumors.

PITUITARY HYPERPLASIA
Pituitary hyperplasia is a nonneoplastic increase in cell number of the anterior pituitary gland. Physiological pituitary hyperplasia is common in pubescent females.[7] Pituitary gland enlargement also occurs during pregnancy. Pathological hyperplasia often occurs in response to target organ failure. MRI reveals a diffuse enhanced symmetric lesion in the sellar region. For example, long-standing untreated primary hypothyroidism can cause pituitary hyperplasia owing to hormonal-feedback mechanisms. The thyrotropin level normalized and enhanced lesion decreased considerably during thyroxine replacement therapy in most cases (Fig. 1). Pathological hyperplasia, such as growth hormone (GH) or adrenocorticotropic hormone (ACTH) cell hyperplasia, can also be induced by excessive releasing hormones.

Corresponding author: Masamichi Kurosaki, MD, PhD
kurosaki@tottori-u.ac.jp
Received 2021 March 1
Accepted 2021 March 22
Online published 2021 April 16
Abbreviations: ASL, arterial spin-labeled perfusion imaging; CD, Cushing's disease; GH, growth hormone; MRI, magnetic resonance imaging; PRL, prolactin; RCC, Rathke cleft cyst; SE, spin-echo; SPGR, spoiled gradient echo; SWI, susceptibility weighting imaging; T, tesla

© 2021 Tottori University Medical Press

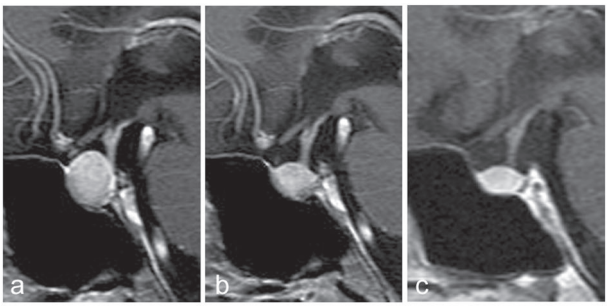

Fig. 1. Sagittal postcontrast T1-weighted MR images of a 55-year-old woman with hypothyroidism during thyroxine replacement therapy. (**a**) Before therapy. A pituitary hyperplasia is visible as an enhanced lesion. (**b**) At 5 months. (**c**) At 18 months. The enhanced lesion has decreased considerably.

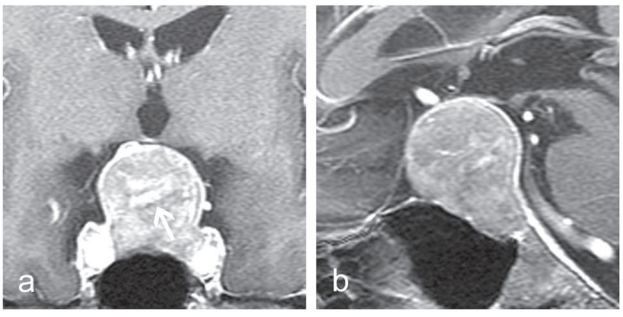

Fig. 2. Postcontrast T1-weighted MR images of a 61-year-old man with a non-functioning fibrous macroadenoma. An arrow indicates brushed enhancement. (**a**) Coronall view (**b**) Sagittal view.

PITUITARY ADENOMA

Adenomas 10 mm in diameter or more are defined as macroadenomas, which are easily diagnosed; however, they require careful delineation. In our previous study,[3] 3T MRI, particularly three dimensional (3D)-spoiled gradient echo (SPGR) sequence demonstrated the defined relationship between the tumor and its surroundings, such as the normal pituitary gland, cavernous sinus, and optic pathway. The pituitary gland enhances homogeneously, whereas the microadenoma enhances afterwards; therefore, it appears as low signal intensity on postcontrast T1weighted image (WI).

Pituitary adenomas are usually soft and easy to excise by aspiration or curettage. However, fibrous adenomas are more difficult to excise and occur with a certain incidence. Predicting fibrous adenomas by MRI is typically difficult and unreliable. We proposed that brushed enhancement was one of the reliable findings for fibrous hyperperfusion adenoma. Subsequently, this brushed enhancement of fibrous adenomas was identified clearly on postcontrast T1WI (Fig. 2). Intratumoral flow void, indicating the inferior hypophyseal artery, was demonstrated clearly on T2WI in some hypervascular cases. In our study, intratumoral flow void was depicted clearly in nine of 72 cases (12.5%) on T2WI. Recently, we have performed arterial spin-labeled perfusion imaging (ASL) to measure the blood flow of pituitary macroadenomas preoperatively. ASL is an MRI technique for perfusion measurement. This technique requires no extrinsic tracer, such as gadolinium chelates. Instead, it uses electromagnetically labeled arterial blood water as an intrinsic tracer. Sakai et al. reported that ASL was useful in the preoperative prediction of intra- and postoperative tumor hemorrhage, consistent with our study findings.[8]

The incidence of hemorrhage within pituitary adenoma, so called pituitary apoplexy, ranges between 1.9% and 26.5%.[9–11] Asymptomatic pituitary apoplexy is being frequently diagnosed owning to recent advances in MRI. In our study, in four of 17 cases, hemorrhage was detected in pituitary adenomas by susceptibility WI, but not by T2WI. We suggest that susceptibility WI should be used to provide diagnostic assistance for pituitary apoplexy.[12]

Pituitary adenomas are clinically classified into two groups, namely, functioning and non-functioning adenomas. The characteristic MRI findings of functioning pituitary adenoma, such as ACTH, GH, and prolactin (PRL)-producing adenoma, are reviewed.

Approximately 90% of pituitary adenomas causing Cushing's disease (CD) are microadenomas with a diameter of less than 10 mm. As adenomas of 5 mm or less are frequent, a large percentage of these microadenomas cannot be visualized by high resolution MRI.[13] Transsphenoidal surgery is the first-choice treatment for CD. The surgical cure rate for CD is approximately 80–90% when a tumor is visible on MRI.[14] It decreases to 50–70% when the lesion cannot be localized on MRI.[14] Correct localization of the tumor on MRI helps in improving the surgical cure rate. Although many authors advocate dynamic study as a technique to increase sensitivity to microadenomas, the spatial resolution of dynamic contrast-enhanced MRI is poor. Patronas et al. recommend the addition of SPGR sequences characterized by superior soft tissue contrast using pituitary-specific technical parameters to improve the MRI detection of ACTH-secreting pituitary tumors.[15] Volume interpolated 3D-spoiled gradient MRI sequence, which is similar to SPGR sequence, is better for localization of pituitary microadenomas in CD than dynamic contrast SE sequence.[16] We also propose that 3D-SPGR sequence is the more suitable sequence for detecting the microadenoma using the current state-of-the-art high-field MRI (Fig. 3).

© 2021 Tottori University Medical Press

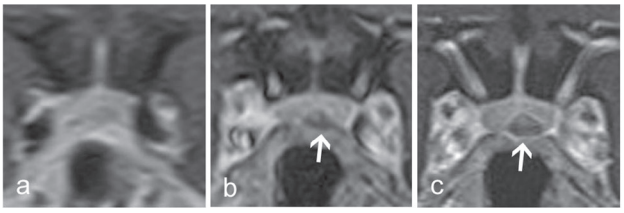

Fig. 3. Coronal T1-weighted MR images of the sellar region of a 15-year-old man with ACTH-producing pituitary microadenoma. (**a**) 1.5T dynamic (**b**) 1.5T 3D-grdient echo sequence (**c**) 3T 3D-SPGR sequence. The 3D-SPGR 3T MR images are superior to the other images for visualization of the microadenoma (arrows).

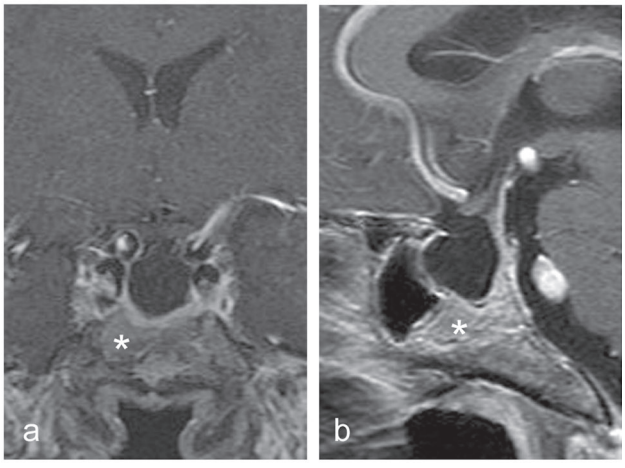

Fig. 4. Postcontrast T1-weighted MR images of a 64-year-old woman with acromegaly. (**a**) Coronall view (**b**) Sagittal view. This patient was transferred to our hospital for the treatment of intracranial hemorrhage owning to hypertension. A diagnosis of acromegaly was suspected from the clinical features. However, the pituitary adenoma could not be detected. Postcontrast T1WI revealed a macroadenoma (*) invading into the sphenoid sinus inferiorly during the radiological examination.

Transsphenoidal surgery is the first-choice treatment for acromegaly. Unless the patients have achieved endocrinological remission after surgery, medical and/or radiation therapy should be considered. Somatostatin analogues represent the first-choice medical treatment for acromegaly. Numerous factors are associated with resistance somatostatin analogues, including sparsely granulated adenoma subtype. The sparsely granulated adenoma is more aggressive tumor. Predicting treatment response of somatostatin analogues is necessary, and signal intensity on T2WI may improve preoperative classification of GH-producing adenomas.[17] Characteristic features of GH-producing pituitary adenomas have been reported. For example, GH-producing adenomas tend to demonstrate infrasellar extension (Fig. 4). Empty sella is also associated in some cases. In GH-producing adenomas, T2-weighted MRI signal intensity is a marker for granulation pattern. Hypointense is almost exclusive for densely granulated adenomas.[18] Sparsely granulated adenoma has relatively hyperintense mass. Using 3T MRI the border of densely granulated GH-producing adenomas and tumor contents is identified more clearly on T2WI. The pituitary adenoma is depicted clearly as a less enhanced area surrounding the normal pituitary gland on postcontrast T1WI (Fig. 5). We propose that T2-weighted and postcontrast SPGR T1-weighted images are suitable sequences for evaluating GH-producing pituitary adenomas at 3T.

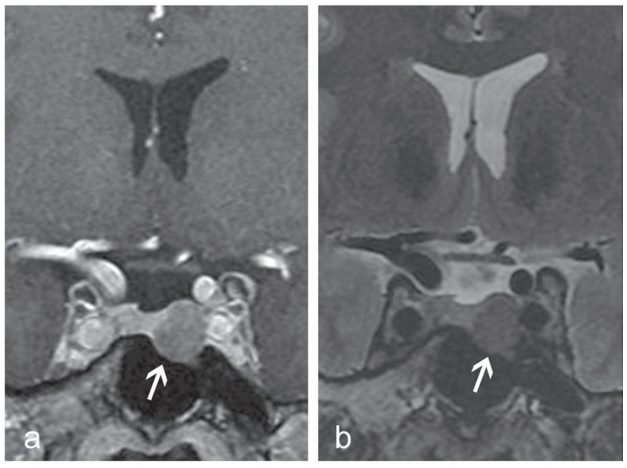

Fig. 5. Postcontrast coronal T1-weighted (**a**), and T2-weighted (**b**) MR images of the sellar region of a 42-year-old man with a GH-producing pituitary adenoma (densely granulated type). The adenoma is clearly visible as a low signal intense mass (arrows). The tumor was excised entirely by the endonasal approach. Histopathological diagnosis of a densely granulated somatotroph adenoma was established.

Cabergoline has been widely accepted as the primary treatment for PRL-producing pituitary adenomas, because it has higher efficacy in normalizing PRL levels and reducing tumor mass.[19, 20] Although a high percentage rate of tumor shrinkage was reported, tumors completely disappeared on MRI in only approximately 20% of cases.[21] During treatment with dopamine agonist, variable MRI characteristics have been observed. We reported distinct low signal intensity areas on T2WI in early phase of treatment, possibly owning to diffuse hemorrhage, which indicated pronounced regressions of PRL-producing pituitary adenomas during cabergoline treatment (Fig. 6).[22]

CRANIOPHARYNGIOMA

Craniopharyngiomas are sellar and/or suprasellar masses that derive from epithelial remnants of the Rathke's pouch. Although histologically benign, these

© 2021 Tottori University Medical Press

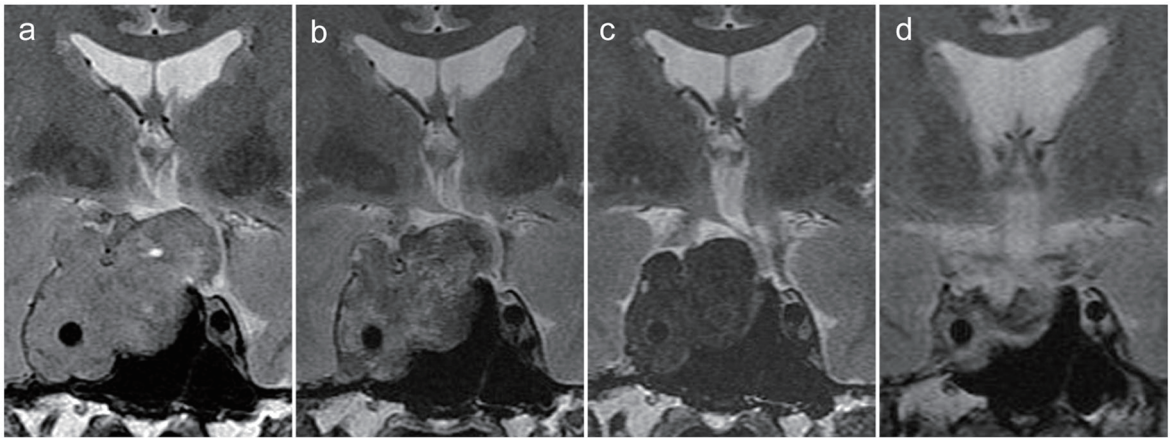

Fig. 6. Coronal T2-weighted MR images of the sellar region of a 37-year-old man with a PRL-producing adenoma during cabergoline treatment. This patient was referred to our hospital, complaining of a headache and visual disturbance. Cabergoline treatment was initiated as the serum PRL was over 470 ng/mL. Tumor size has decreased considerably. (**a**) Before therapy, a macroadenoma is visible as a high signal intensity area. (**b**) At 4 months, a low signal intensity area, possibly owning to diffuse hemorrhage, has developed throughout the adenoma. Thereafter, the tumor decreased considerably in size. (**c**) At 1 year, the formerly low signal intensity region has transformed into a high signal intensity area slightly. (**d**) At 3 years, intracavernous sinus area finally demonstrates high signal intensity.

tumors frequently recur after surgery. The two histopathological subtypes, adamantinomatous and squamous papillary craniopharyngioma, differ in genesis and age distribution.[23] On MRI, these lesions have a heterogenous appearance with a solid portion and cystic components. The typical appearance of adamantinomatous craniopharyngioma is multilobulated and partially solid; however, they are mostly a cystic suprasellar mass (Fig. 7). The cysts often contain "machinery oil" fluid. Calcified tumors are mostly of the adamantinomatous type. Characteristic rim and nodular calcifications are best detected on computed tomography. Squamous papillary craniopharyngioma is a typically discrete encapsulated tumor with a smooth surface that does not adhere to the adjacent brain. The cysts contain clear fluid. Recent insights into the molecular pathogenesis of craniopharyngiomas opened new perspectives on targeted therapy in squamous papillary craniopharyngioma harboring BRAF-V600E mutations. Adamantinomatous craniopharyngiomas are driven by somatic mutations in CTNNB1 (encoding β-catenin).

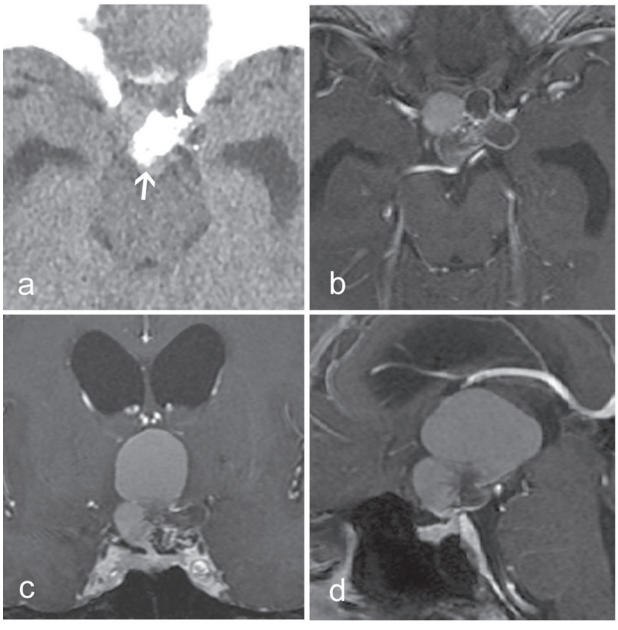

Fig. 7. Precontrast CT (**a**) and postcontrast MR images (**b**, **c**, **d**) of the sellar region of a 47-year-old woman with craniopharyngioma. Chunky and irregular calcification (arrow) of the suprasellar mass is more clearly visible on CT rather than MRI. MR images depicts the solid and cystic mass clearly.

RATHKE CLEFT CYST

Rathke cleft cysts (RCCs) are benign sellar and/or suprasellar cysts that arise from the remnants of Rathke's pouch. Signal intensity varies with cyst contents. RCCs of high- and iso signal intensity on T1WI, which contain mucous material, may be associated with chronic inflammation that can potentially cause irreversible endocrine dysfunction.[24] However, patients with low signal intensity content tend to experience visual disturbances.[24] Although cyst fluid of RCC shows variable intensities on MRI, intracystic waxy nodule is hypointense on T2WI (Fig. 8).[25] The enhancing cyst wall may contain the squamous metaplasia. Symptomatic RCCs are mostly treated by draining the cyst contents with partial removal of the cyst wall. The

© 2021 Tottori University Medical Press

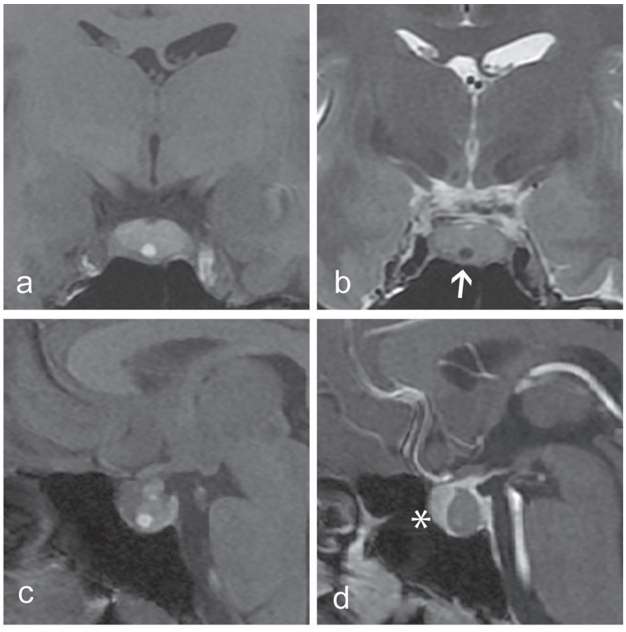

Fig. 8. Precontrast T1-weighted (**a**, **c**), T2-weighted (**b**), and postcontrast T1-weighted images (**d**) of the sellar region of a 36-year-old woman with a Rathke cleft cyst. Mural waxy nodule is clearly visible as a low signal intense mass (arrow). The cyst is situated between anterior (*) and posterior pituitary gland.

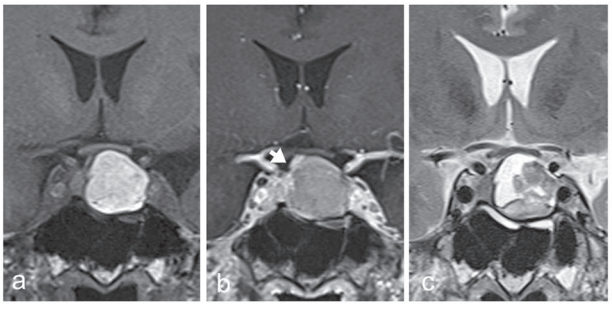

Fig. 9. Coronal precontrast T1-weighted (**a**), postcontrast T1 weighted (**b**), and T2-weighted (**c**) MR images of a 60-year-old man with a xanthogranuloma of the sellar region. Thin enhanced lesion is formed by a thin rim of compressed pituitary gland and stalk (arrow). Cyst contents show variable signal intensity on T2WI. Hemosiderin rim are detected.

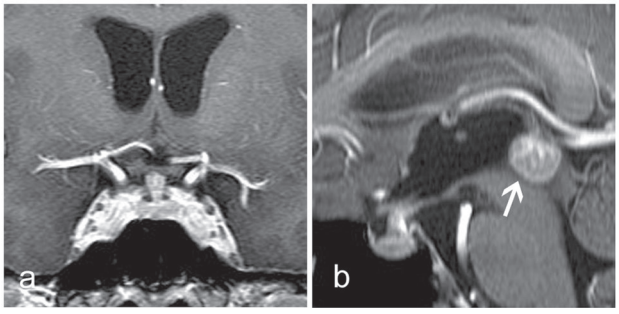

Fig. 10. Postcontrast T1-weighted MR images of a 42-year-old man with a germ cell tumor. (**a**) Coronall view. A swollen pituitary stalk is visible as an enhanced lesion. (**b**) Sagittal view. A pineal lesion (arrow) is also present.

reported recurrence rates have ranged between 10% and 42%, a relatively high percentage. The presence of squamous metaplasia in the cyst wall was associated with the recurrence after surgery.[26, 27] Spontaneous regression of RCC may not be rare after presenting with severe headache.[28]

XANTHOGRANULOMA OF THE SELLAR REGION

Paulus et al. suggest that xanthogranuloma of the sellar region is clinically and pathologically different from the classical adamantinomatous craniopharyngioma.[29] In 2000, the World Health Organization accepted xanthogranuloma of the sellar region as a distinct entity. These lesions consist largely of cholesterol clefts, macrophages, and chronic inflammatory infiltrates without epithelium. Typical radiological findings have not been reported yet. These lesions show variable signal intensity on T2WI in our experience. Most are high signal intensities on T1WI. Hemosiderin rims are found in some cases (Fig. 9).

Cystic lesions of the sellar and/or parasellar areas are difficult to differentiate on clinical, imaging, or even a histopathological basis. Several varieties of "transitional" or "crossover" cystic epithelial lesions have been reported in the literature.[30] One of them is RCC with squamous metaplasia. The higher recurrence rates observed in these cases support the idea that they likely show more aggressive behavior. Ciliated craniopharyngioma is also considered to represent a transitional stage between RCC and squamous papillary craniopharyngioma.[30]

NEUROHYPOPHYSEAL GERMINOMA

Germ cell tumors are divided into two groups, namely germinoma and nongerminomatous germ cell tumors. Germ cell tumors tend to occur at the midline, such as the neurohypophysis, around the third ventricle, and pineal region.[31] Synchronous intracranial germ cell tumor in the pineal and neurohypophyseal region is rare (Fig. 10). Infundibular thickening and absence of the posterior pituitary high signal intensity spot on T1WI are common imaging features of neurohypophyseal germinoma. Recently, Morana et al. reported that all nongerminomatous germ cell tumors showed susceptibility WI or T2WI hypointensity, whereas all but one pure germinoma were isointense or hyperintense among midline germ cell tumor.[32] Subsequently,

© 2021 Tottori University Medical Press

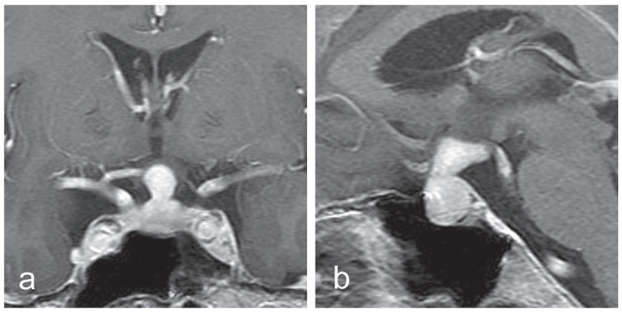

Fig. 11. Postcontrast T1-weighted MR images of a 66-year-old man with lymphocytic hypophysitis. A swollen pituitary stalk is visible as an enhanced lesion. (**a**) Coronall view (**b**) Sagittal view.

they recommend the T2*-based MRI in differentiating pure germinomas from nongerminomatous germ cell tumors.

LYMPHOCYTIC HYPOPHYSITIS

Primary hypophysitis is classified by histologic appearance as lymphocytic, granulomatous, xanthomatous, immunoglobulin G4 plasmacytic,[33] and mixed form. Lymphocytic hypophysitis is an inflammatory disorder of the pituitary gland, which occurs in the adenohypophysis and/or infundibulo-neurohypophysis.[34, 35] Lymphocytic hypophysitis is often misdiagnosed because its clinical and radiological features mimic tumors in the sellar region. When the inflammatory process is limited to the infundibulo-neurohypophysis, infundibular thickening and absence of the posterior pituitary high signal intensity spot are common on T1WI (Fig. 11). Differentiation from other stalk lesions, such as germinoma and Langerhans cell histiocytosis, may be difficult. Dark-signal intensity areas on T2WI around the pituitary gland and in the cavernous sinus, namely the parasellar T2 dark sign was reported as a characteristic feature useful for distinguishing pituitary adenoma from this disease in patients with lymphocytic hypophysitis.[36]

CONCLUSION

Our clinical experience with 3T MR images was reported with emphasis on hypothalamic and pituitary tumors. Because of the high signal-to-noise ratio, 3T MRI was superior to 1.5T MRI in visualization of tumors, as well as the surroundings. Especially, T2WI and postcontrast SPGR T1WI provide high anatomical and contrast resolution. These images demonstrate the defined relationship between the tumor and its surroundings, such as the normal pituitary gland, the cavernous sinus, and the optic pathway.

The authors declare no conflict of interest.

REFERENCES

1 Maya MM, Pressman BD. Pituitary imaging. In: Melmed S, editor. The pituitary, 3rd ed. San Diego, CA: Academic Press; 2011. p. 677-702.
2 Osborn AG. Sellar neoplasms and tumor-like lesions. In: Renlund AR, editor. Osborn's brain imaging, pathology, and anatomy. Manitoba, Canada: Amirsys Publishing, Inc; 2013. p. 681-771.
3 Kakite S, Fujii S, Kurosaki M, Kanasaki Y, Matsusue E, Kaminou T, et al. Three-dimensional gradient echo versus spin echo sequence in contrast-enhanced imaging of the pituitary gland at 3T. Eur J Radiol. 2011;79:108-12. DOI: 10.1016/j.ejrad.2009.12.036, PMID: 20116954
4 Pinker K, Ba-Ssalamah A, Wolfsberger S, Mlynarik V, Knosp E, Trattnig S. The value of high-field MRI (3T) in the assessment of sellar lesions. Eur J Radiol. 2005;54:327-34. DOI: 10.1016/j.ejrad.2004.08.006, PMID: 15899332
5 Wolfsberger S, Ba-Ssalamah A, Pinker K, Mlynárik V, Czech T, Knosp E, et al. Application of three-tesla magnetic resonance imaging for diagnosis and surgery of sellar lesions. J Neurosurg. 2004;100:278-86. DOI: 10.3171/jns.2004.100.2.0278, PMID: 15086236
6 Haacke EM, Xu Y, Cheng YCN, Reichenbach JR. Susceptibility weighted imaging (SWI). Magn Reson Med. 2004;52:612-8. DOI: 10.1002/mrm.20198, PMID: 15334582
7 Elster AD, Chen MY, Williams DW III, Key LL. Pituitary gland: MR imaging of physiologic hypertrophy in adolescence. Radiology. 1990;174:681-5. DOI: 10.1148/radiology.174.3.2305049, PMID: 2305049
8 Sakai N, Koizumi S, Yamashita S, Takehara Y, Sakahara H, Baba S, et al. Arterial spin-labeled perfusion imaging reflects vascular density in nonfunctioning pituitary macroadenomas. AJNR Am J Neuroradiol. 2013;34:2139-43. DOI: 10.3174/ajnr.A3564, PMID: 23721898
9 Kurihara N, Takahashi S, Higano S, Ikeda H, Mugikura S, Singh LN, et al. Hemorrhage in pituitary adenoma: correlation of MR imaging with operative findings. Eur Radiol. 1998;8:971-6. DOI: 10.1007/s003300050498, PMID: 9683703
10 Onesti ST, Wisniewski T, Post KD. Clinical versus subclinical pituitary apoplexy: presentation, surgical management, and outcome in 21 patients. Neurosurgery. 1990;26:980-6. DOI: 10.1227/00006123-199006000-00010, PMID: 2362675
11 Wakai S, Fukushima T, Teramoto A, Sano K. Pituitary apoplexy: its incidence and clinical significance. J Neurosurg. 1981;55:187-93. DOI: 10.3171/jns.1981.55.2.0187, PMID: 7252541
12 Kurosaki M, Tabuchi S, Akatsuka K, Kamitani H, Watanabe T. Application of phase sensitive imaging (PSI) for hemorrhage diagnosis in pituitary adenomas. Neurol Res. 2010;32:614-9. DOI: 10.1179/174313209X455709, PMID: 19660234
13 Colao A, Boscaro M, Ferone D, Casanueva FF. Managing Cushing's disease: the state of the art. Endocrine. 2014;47:9-20. DOI: 10.1007/s12020-013-0129-2, PMID: 24415169
14 Yamada S, Fukuhara N, Nishioka H, Takeshita A, Inoshita N, Ito J, et al. Surgical management and outcomes in patients with Cushing disease with negative pituitary magnetic resonance imaging. World Neurosurg. 2012;77:525-32. DOI: 10.1016/j.wneu.2011.06.033, PMID: 22120352

© 2021 Tottori University Medical Press

15 Patronas N, Bulakbasi N, Stratakis CA, Lafferty A, Oldfield EH, Doppman J, et al. Spoiled gradient recalled acquisition in the steady state technique is superior to conventional post-contrast spin echo technique for magnetic resonance imaging detection of adrenocorticotropin-secreting pituitary tumors. J Clin Endocrinol Metab. 2003;88:1565-9. DOI: 10.1210/jc.2002-021438, PMID: 12679440
16 Kasaliwal R, Sankhe SS, Lila AR, Budyal SR, Jagtap VS, Sarathi V, et al. Volume interpolated 3D-spoiled gradient echo sequence is better than dynamic contrast spin echo sequence for MRI detection of corticotropin secreting pituitary microadenomas. Horumon To Rinsho. 2013;78:825-30. DOI: 10.1111/cen.12069, PMID: 23061773
17 Heck A, Emblem KE, Casar-Borota O, Bollerslev J, Ringstad G. Quantitative analyses of T2-weighted MRI as a potential marker for response to somatostatin analogs in newly diagnosed acromegaly. Endocrine. 2016;52:333-43. DOI: 10.1007/s12020-015-0766-8, PMID: 26475495
18 Hagiwara A, Inoue Y, Wakasa K, Haba T, Tashiro T, Miyamoto T. Comparison of growth hormone-producing and non-growth hormone-producing pituitary adenomas: imaging characteristics and pathologic correlation. Radiology. 2003;228:533-8. DOI: 10.1148/radiol.2282020695, PMID: 12819334
19 Casanueva FF, Molitch ME, Schlechte JA, Abs R, Bonert V, Bronstein MD, et al. Guidelines of the Pituitary Society for the diagnosis and management of prolactinomas. Horumon To Rinsho. 2006;65:265-73. DOI: 10.1111/j.1365-2265.2006.02562.x, PMID: 16886971
20 Melmed S, Casanueva FF, Hoffman AR, Kleinberg DL, Montori VM, Schlechte JA, et al.; Endocrine Society. Diagnosis and treatment of hyperprolactinemia: an Endocrine Society clinical practice guideline. J Clin Endocrinol Metab. 2011;96:273-88. DOI: 10.1210/jc.2010-1692, PMID: 21296991
21 Colao A, Di Sarno A, Landi ML, Scavuzzo F, Cappabianca P, Pivonello R, et al. Macroprolactinoma shrinkage during cabergoline treatment is greater in naive patients than in patients pretreated with other dopamine agonists: a prospective study in 110 patients. J Clin Endocrinol Metab. 2000;85:2247-52. DOI: 10.1210/jc.85.6.2247, PMID: 10852458
22 Kurosaki M, Kambe A, Watanabe T, Fujii S, Ogawa T. Serial 3 T magnetic resonance imaging during cabergoline treatment of macroprolactinomas. Neurol Res. 2015;37:341-6. DOI: 10.1179/1743132814Y.0000000457, PMID: 25376133
23 Brastianos PK, Taylor-Weiner A, Manley PE, Jones RT, Dias-Santagata D, Thorner AR, et al. Exome sequencing identifies BRAF mutations in papillary craniopharyngiomas. Nat Genet. 2014;46:161-5. DOI: 10.1038/ng.2868, PMID: 24413733
24 Nishioka H, Haraoka J, Izawa H, Ikeda Y. Magnetic resonance imaging, clinical manifestations, and management of Rathke's cleft cyst. Horumon To Rinsho. 2006;64:184-8. DOI: 10.1111/j.1365-2265.2006.02446.x, PMID: 16430718
25 Binning MJ, Gottfried ON, Osborn AG, Couldwell WT. Rathke cleft cyst intracystic nodule: a characteristic magnetic resonance imaging finding. J Neurosurg. 2005;103:837-40. DOI: 10.3171/jns.2005.103.5.0837, PMID: 16304987
26 Aho CJ, Liu C, Zelman V, Couldwell WT, Weiss MH. Surgical outcomes in 118 patients with Rathke cleft cysts. J Neurosurg. 2005;102:189-93. DOI: 10.3171/jns.2005.102.2.0189, PMID: 15739543
27 Benveniste RJ, King WA, Walsh J, Lee JS, Naidich TP, Post KD. Surgery for Rathke cleft cysts: technical considerations and outcomes. J Neurosurg. 2004;101:577-84. DOI: 10.3171/jns.2004.101.4.0577, PMID: 15481709
28 Amhaz HH, Chamoun RB, Waguespack SG, Shah K, McCutcheon IE. Spontaneous involution of Rathke cleft cysts: is it rare or just underreported? J Neurosurg. 2010;112:1327-32. DOI: 10.3171/2009.10.JNS091070, PMID: 19929199
29 Paulus W, Honegger J, Keyvani K, Fahlbusch R. Xanthogranuloma of the sellar region: a clinicopathological entity different from adamantinomatous craniopharyngioma. Acta Neuropathol. 1999;97:377-82. DOI: 10.1007/s004010051001, PMID: 10208277
30 Zada G, Lin N, Ojerholm E, Ramkissoon S, Laws ER. Craniopharyngioma and other cystic epithelial lesions of the sellar region: a review of clinical, imaging, and histopathological relationships. Neurosurg Focus. 2010;28:E4. DOI: 10.3171/2010.2.FOCUS09318, PMID: 20367361
31 Fujisawa I, Asato R, Okumura R, Nakano Y, Shibata T, Hamanaka D, et al. Magnetic resonance imaging of neurohypophyseal germinomas. Cancer. 1991;68:1009-14. DOI: 10.1002/1097-0142(19910901)68:5<1009::AID-CNCR2820680517>3.0.CO;2-R, PMID: 1913472
32 Morana G, Alves CA, Tortora D, Finlay JL, Severino M, Nozza P, et al. T2*-based MR imaging (gradient echo or susceptibility-weighted imaging) in midline and off-midline intracranial germ cell tumors: a pilot study. Neuroradiology. 2018;60:89-99. DOI: 10.1007/s00234-017-1947-3, PMID: 29128947
33 Shikuma J, Kan K, Ito R, Hara K, Sakai H, Miwa T, et al. Critical review of IgG4-related hypophysitis. Pituitary. 2017;20:282-91. DOI: 10.1007/s11102-016-0773-7, PMID: 27812776
34 Levine SN, Benzel EC, Fowler MR, Shroyer JV III, Mirfakhraee M. Lymphocytic adenohypophysitis: clinical, radiological, and magnetic resonance imaging characterization. Neurosurgery. 1988;22:937-41. DOI: 10.1227/00006123-198805000-00025, PMID: 3380286
35 Imura H, Nakao K, Shimatsu A, Ogawa Y, Sando T, Fujisawa I, et al. Lymphocytic infundibuloneurohypophysitis as a cause of central diabetes insipidus. N Engl J Med. 1993;329:683-9. DOI: 10.1056/NEJM199309023291002, PMID: 8345854
36 Nakata Y, Sato N, Masumoto T, Mori H, Akai H, Nobusawa H, et al. Parasellar T2 dark sign on MR imaging in patients with lymphocytic hypophysitis. AJNR Am J Neuroradiol. 2010;31:1944-50. DOI: 10.3174/ajnr.A2201, PMID: 20651017

© 2021 Tottori University Medical Press